Medicine®

OBSERVATIONAL STUDY

OPEN

Association Between Autonomic Impairment and Structural Deficit in Parkinson Disease

Meng-Hsiang Chen, MD, Cheng-Hsien Lu, MD, MS, Pei-Chin Chen, MS, Nai-Wen Tsai, MD, PhD, Chih-Cheng Huang, MD, PhD, Hsiu-Ling Chen, MD, I-Hsiao Yang, MD, Chiun-Chieh Yu, MD, and Wei-Che Lin, MD, PhD

Abstract: Patients with Parkinson disease (PD) have impaired autonomic function and altered brain structure. This study aimed to evaluate the relationship of gray matter volume (GMV) determined by voxel-based morphometry (VBM) to autonomic impairment in patients with PD.

Whole-brain VBM analysis was performed on 3-dimensional T1-weighted images in 23 patients with PD and 15 sex- and age-matched healthy volunteers. The relationship of cardiovascular autonomic function (determined by survey) to baroreflex sensitivity (BRS) (determined from changes in heart rate and blood pressure during the early phase II of the Valsalva maneuver) was tested using least-squares regression analysis. The differences in GMV, autonomic parameters, and clinical data were correlated after adjusting for age and sex.

Compared with controls, patients with PD had low BRS, suggesting worse cardiovascular autonomic function, and smaller GMV in several brain locations, including the right amygdala, left hippocampal formation, bilateral insular cortex, bilateral caudate nucleus, bilateral cerebellum, right fusiform, and left middle frontal gyri. The decreased GMVs of the selected brain regions were also associated with increased presence of epithelial progenitor cells (EPCs) in the circulation.

In patients with PD, decrease in cardiovascular autonomic function and increase in circulating EPC level are associated with smaller GMV in several areas of the brain. Because of its possible role in the modulation of the circulatory EPC pool and baroreflex control, the left hippocampal formation may be a bio-target for disease-modifying therapy and treatment monitoring in PD.

(*Medicine* 95(11):e3086)

Abbreviations: BRS = baroreflex sensitivity, EPC = epithelial progenitor cell, GMV = gray matter volume, HF = high frequency, HRDB = heart rate response to deep breathing, LF = low frequency, modified H&Y = modified Hoehn and Yahr staging, PD = Parkinson disease, S&E = Schwab and England activities of daily living, UPDRS = Unified Parkinson Disease Rating Scale, VBM = voxel-based morphometry, VLF = very low frequency, VRV = alsalva ratio.

INTRODUCTION

Autonomic nervous system dysfunction is a common[1] and progressive[2] manifestation of Parkinson disease (PD). Unfortunately, this dysfunction can become a life-threatening condition.[2] Baroreflex sensitivity (BRS) testing has gained recent popularity as a means of investigating autonomic nervous system activity in PD.[3] Autoregressive analysis of cyclic fluctuations in R–R intervals (R–R interval variability) produces power spectra, portions of which reflect autonomic influences on heart rate and blood pressure.[4] Research suggests that the relative change in autonomic activity (e.g., R–R interval variability dysregulation characterized by increased sympathetic and decreased parasympathetic activity in response to stress) may signal the presence of cardiovascular comorbidities.[3]

The causes of autonomic dysfunction in PD appear to be related to the peripheral nervous system.[5] Cardiac sympathetic denervation is observed in the early stage of PD and progresses as the disease progresses and as aggregates of abnormal α-synuclein form in the epicardial nerve fascicles.[5] But the pathological findings of PD suggest vulnerability in both the peripheral and the central nervous systems.[6] Autonomic dysfunction in PD may be linked to regional brain stem atrophy.[7] However, the relationship between cardiovascular dysfunction and altered brain structure is still unclear.

PD primarily results from the loss of nigrostriatal dopaminergic neurons, which leads to striatal dopamine deafferentation[8] followed by degeneration of other nondopaminergic systems such as the extrapyramidal system.[3] A meta-analysis of voxel-based morphometry (VBM) studies showed brain structure damage in the medial temporal lobe, caudate, lentiform, thalamus, insula, middle frontal gyrus, and limbic system.[9,10] Also, some studies show that gray matter volume (GMV) changes as autonomic dysfunction increases in certain diseases.[11–13] Pathophysiological studies[8,14] and functional imaging studies[15] of PD also reveal the involvement of cortico-basal ganglia-thalamocortical circuits in the mediation of PD symptoms. However, the relationship between autonomic deficits and damage to vulnerable neurological structures in PD remains ill-defined.

Also unclear is the etiology of autonomic dysfunction in PD. Recently, cardiovascular autonomic dysfunction was linked to oxidative stress in an animal model,[16] and oxidative stress

Editor: Mohammad Haris.
Received: November 10, 2015; revised: February 3, 2016; accepted: February 10, 2016.
From the Departments of Diagnostic Radiology (M-HC, P-CC, H-LC, I-HY, C-CY, W-CL) and Neurology (C-HL, N-WT, C-CH), Kaohsiung Chang Gung Memorial Hospital, Chang Gung University College of Medicine; Department of Biological Science, National Sun Yat-Sen University (C-HL), Kaohsiung; and Department of Biomedical Imaging and Radiological Sciences, National Yang-Ming University, Taipei (H-LC), Taiwan.
Correspondence: Wei-Che Lin, Department of Diagnostic Radiology, Kaohsiung Chang Gung Memorial Hospital, Chang Gung University College of Medicine, 123 Ta-Pei Road, Niao-Sung, Kaohsiung 83305, Taiwan (e-mail: u64lin@yahoo.com.tw).
This work was supported by funds from the National Science Council (MOST 103-2314-B-182A-010-MY3 to W-CL and MOST 104-2314-B-182A-053 to H-LC) and Chang Gung Memorial Hospital (CMRPG891511 and CMRPG8B0831 to W-CL, CMRPG890801 and CMRPG8C0021 to H-LC, and CMRPG8E0621 to M-HC).
The authors have no conflicts of interest to disclose.

ISSN: 0025-7974
DOI: 10.1097/MD.0000000000003086

and inflammation were found to play roles in PD pathogenesis.[17] Moreover, factors secreted by endothelial progenitor cells (EPCs) were shown to protect against oxidative stress; to participate in differentiation to neural progenitor cells, neovascularization, and cognitive impairment after stroke[18,19]; and to repair and form new blood vessels under the neurodegenerative conditions of stroke.[20,21] Nevertheless, the relationship of EPCs to autonomic dysfunction and regional brain atrophy is not fully understood.

Based on previous findings, we propose that autonomic activity is lower, circulating EPC level is higher, and regional GMV, smaller, in patients with PD (compared with controls); and an decreased autonomic function and increased EPC level are associated with regional GMV reduction.

METHODS

Participants

The study protocol was approved by the Local Ethics Committee on Human Research of Kaohsiung Chang Gung Memorial Hospital in Taiwan (IRB 102-5255A3). All participants or their guardians provided written informed consent prior to participation in the study. Twenty-three patients (6 men and 17 women, mean age: 61.0 ± 6.8 years) with no previous history of neurological or psychiatric illnesses, psychotropic medication, or contraindication to magnetic resonance imaging (MRI) were prospectively enrolled at the Neurology Department of Kaohsiung Chang Gung Memorial Hospital. Patients were included if they had idiopathic PD diagnosed by an experienced neurologist according to the Parkinson Disease Society's criteria.[22] The disease severity and functional status of each patient were evaluated on the Unified Parkinson Disease Rating Scale (UPDRS),[23] modified Hoehn and Yahr staging (H&Y) scale,[24] and the Schwab and England (S&E) activities of daily living scale[25] in the ''OFF'' state, that is, after levodopa-induced suppression of motor symptoms has worn off, leaving patients unable to function properly. The UPDRS is the scale most commonly used to follow the longitudinal course of PD, and it is evaluated via interview and clinical observation. The UPDRS was developed as a compound scale to capture multiple aspects of PD including both motor disability (Part II: Activities of daily living) and motor impairment (Part III) as well as mental dysfunction and mood (Part I), and treatment-related motor and nonmotor complications (Part IV). The modified H&Y scale provides a global measure of functional disability based on clinical findings. It is commonly used to track the progression of PD from stages 1 through 5, with later stages being more severe. The S&E scale estimates the abilities of patients with PD relative to completely healthy and independent individuals. A score of 100% indicates a completely independent patient, while a score of 0% indicates a bedridden individual with only vegetative functions.

For comparison, 15 sex- and age-matched healthy subjects (5 men and 10 women, mean age: 56.0 ± 9.0 years) were recruited with no medical history of neurologic diseases or psychiatric illnesses, alcohol/substance abuse, or head injury, and with similar levels of education.

Cardiovascular Autonomic Parameters

Heart rate was derived from continuously recorded standard 3-lead electrocardiogram (Ivy Biomedical, model 3000; Branford, CT) while arterial blood pressure was continuously measured using beat-to-beat photoplethysmographic recordings (Finameter Pro, Ohmeda, Englewood, OH). Testworks software (WR Medical Electronics Company, Stillwater, MN) was used to determine the heart rate response to deep breathing (HRDB), Valsalva ratio, and BRS, which was determined by least-squares regression analysis of changes in HR and blood pressure occurring during the early phase II of the Valsalva maneuver.

Beat-to-beat R–R interval changes were interpolated using a 3rd-order polynomial and were re-sampled every 0.5 s. The signals (512 samples) were then fast Fourier transformed to the frequency domain. Spectral powers were divided into 3 frequency domains: high frequency (HF, 0.15–0.4 Hz), low frequency (LF, 0.04–0.15 Hz), and very LF (0.00–0.04 Hz). The ratio between powers of LF and HF (LF/HF ratio) was taken as an index of sympatho-vagal balance.

MR Image Acquisition

Volumetric structural MRI scans were acquired on a GE Signa 3T whole-body MRI scanner (General Electric Healthcare, Milwaukee, WI) using an 8-channel phase array head coil at the Kaohsiung Chang Gung Memorial Hospital in Taiwan. Whole brain 3-dimensional T1-weighted images were collected using an inversion-recovery fluid-attenuated fast spoiled gradient-recalled echo pulse sequence. In all, 110 contiguous axial slices were aligned to the anterior and posterior commissure and acquired with the following imaging parameters for each participant: repetition time (TR)/echo time (TE)/inversion time (TI) = 9.5/3.9/450 ms; flip angle = 15°; number of excitations (NEX) = 1; field of view (FOV) = $240 \times 240\,mm^2$; matrix size = 512×512; and voxel size = $0.47 \times 0.47 \times 1.3\,mm^3$. To identify any brain abnormalities, an additional volumetric axial T2-weighted fast spin-echo sequence (TR/TE = 4200/102 ms; echo train length = 18; NEX = 2; FOV = $240\,mm^2$; slice thickness = 5 mm; matrix size = 320×256 and 18 slices) and axial T2-weighted inversion-recovery fluid-attenuated sequence (TR/TE/TI = 8000/100/2000 ms; NEX = 1; FOV = $240\,mm^2$; slice thickness = 5 mm; matrix size = 320×256 and 18 slices) were used in the same imaging session. To confirm that no participant had morphological abnormalities, all structural MRI scans were visually reviewed by an experienced neuroradiologist who was blinded to participants' disease status. No participant in the study was excluded from this neuroradiological evaluation. The total scanning time for each participant was 20 min.

Circulatory EPCs

To assess circulating EPC number, peripheral blood was sampled and EPC level was measured by flow cytometry. To determine the EPC surface markers of $CD133^+CD34^+$ and KDR^+CD34^+, mononuclear cells were incubated for 30 min at 4°C in a dark room with monoclonal antibodies against kinase insert domain-conjugating receptor (KDR) and CD133 (Miltenyi Biotec, Bergisch Gladbach, Germany), phycoerythrin-conjugated KDR, CD133, and fluorescein isothiocyanate-conjugated CD34 (Beckman Coulter, Fullerton, CA).

A control ligand (IgG-phycoerythrin conjugate) was used to detect any nonspecific association and define a threshold for glycoprotein binding. After staining, the mononuclear cells were fixed in 1% paraformaldehyde. An Epics XL flow cytometer (Beckman Coulter) was used to carry out quantitative 3-color flow cytometry analysis (1,000,000 cells per sample). Intraindividual variability and mean intra-assay coefficients of variance of circulating EPC numbers were all <4.0%.

Data Analysis

Processing Steps in Diffeomorphic Anatomical Registration Through the Exponentiated Lie Algebra (DARTEL)-Based T1 VBM

T1-weighted structural MRI imaging data were analyzed using VBM, the VBM8 toolbox (http://dbm.neuro.uni-jena.de), and the Statistical Parametric Mapping software program (SPM8, Wellcome Institute of Neurology, University College London, UK, http://www.fil.ion.ucl.ac.uk/spm/) with default settings as described in the manual for the VBM8 toolbox. First, all native space T1-weighted structural MRI scan images were bias-corrected and segmented into gray matter (GM), white matter (WM), and cerebrospinal fluid components using the segmentation approach without tissue a priori maps available in the VBM8 toolbox. The VBM8 segmentation included partial volume estimation to account for voxels containing 2 tissue types.[26] The algorithm uses an adaptive Maximum a Posteriori approach (which does not rely on a priori information regarding tissue probabilities[27]) and then a hidden Markov random field model[28] to account for intensity inhomogeneities and variations, without requiring tissue priors for tissue segmentation. By using standard adult reference data as a priori knowledge, this approach avoids introducing systematic bias into the segmentation procedure. To remove the global brain volume differences across subjects while retaining large-scale, inter-individual morphometric variation, these tissue segments were affine registered to the tissue probability maps in the Montreal Neurological Institute (MNI) standard space. After visually checking the affine-registered tissue segments for segmentation errors, the DARTEL toolbox in SPM8 was then used to create a study-specific template made up of the GM and WM segments of all participants. The resulting GM tissue segment images were transformed by the DARTEL registration procedure and interpolated to an isotropic voxel size of 1.5 mm.[29–31] This procedure allowed us to make inferences based on local volumes (relative to overall brain size) rather than on tissue density. Subsequently group comparisons and mediation effects were statistically analyzed and a further quality check routine was implemented in the VBM8 toolbox, using covariance-based inhomogeneity measures of the resulting GM tissue segments. Finally, the resulting MNI space modulated GM segments were smoothed using a Gaussian kernel with full-width at half maximum in 8 mm. The GMV was estimated in cubic millimeters in the native space.

Statistical Analysis

Analysis of Demographic Data, Cardiovascular Autonomic Parameters, Global Tissue Volumes, and Circulating EPCs

The demographic data (including age, sex, and education) were compared among the study groups by the 2-sample Student *t* test and Pearson chi-squared test, where appropriate, and are reported as the mean ± standard deviation (SD). Analysis of covariance (ANCOVA) was used to analyze differences in cardiovascular autonomic parameters and circulatory EPC levels (with the participant's age and sex as covariates) and differences in global tissue volume (with the participant's age, sex, and education as covariates). The *P* value for statistical significance was set at <0.05. All statistical analyses of demographic data and global tissue volumes were performed using SPSS software, version 17, for Windows (SPSS, Chicago, IL).

Voxel-Wise Whole-Brain GMV Comparisons Between Healthy Controls and Patients With PD

To examine between-group differences in GMV, we used a general linear model which was implemented in SPM8 to compare modulated GM segments between healthy controls and patients with PD. A 1-factor 2-level ANCOVA design was utilized to reveal which GMVs were greater in patients than controls and vice versa. To remove the confounding effects of variables known to influence the results of VBM analysis, we entered age, sex, and education as nuisance variables into the ANCOVA model. To further avoid possible partial volume effects around the boundary between GM and WM, all voxels with a GM probability lower than 0.2 were eliminated from the statistical analysis. The resultant statistical inferences were considered significant if the cluster level family-wise error (FWE) corrected *P* value was <0.05, with a cluster size of at least 184 voxels, based on the results of a Monte Carlo simulation (3dClusterSim with the following parameters: single voxel *P* value < 0.005, Full width at half maximum = 7 mm with GM mask and 10,000 simulations). The Peak_nii toolbox (http://www.nitrc.org/projects/peak_nii) was used to assess significant between-group main effects of cluster properties, including cluster size, maximum Z-score, corresponding location of MNI coordinates, and anatomical structure. The clusters with significant group main effects were selected for further mediation analysis.

Correlations Among Demographic Data, Cardiovascular Autonomic Parameters, GMVs, and Circulatory EPC Levels

Partial correlation analysis was used to explore the relationships among demographic data, cardiovascular autonomic parameters, and circulatory EPC levels after controlling for age and sex. To examine the influence of education level on GMVs, partial correlations of GM-related items were demonstrated after controlling age, sex, and education level.

RESULTS

Demographic Data of Participants and Disease Severity of Patients With PD

The demographic and clinical data of the participants are shown in Table 1. The patient and normal control groups had similar mean age and sex distribution (age: $P = 0.214$, and sex: $P = 0.450$). The mean UPDRS I, UPDRS II, UPDRS III, UPDRS total, modified H&Y, and S&E scores were 4.61, 11.78, 28.65, 44.87, 2.41, and 79.57, respectively, for patients with PD.

Between-Group Differences in Cardiovascular Autonomic Parameters

The cardiovascular autonomic parameters of the participants are listed in Table 1. Compared with the normal controls, the patients with PD had significantly decreased BRS (mean ± SD: 8.38 ± 4.10 vs 4.08 ± 2.25; $P = 0.001$) and HRDB (mean ± SD: 11.67 ± 6.89 vs 6.36 ± 3.56; $P = 0.021$). Furthermore, decreased BRS was associated with higher UPDRS III score indicating increased disease severity ($r = -0.443$, $P = 0.044$).

Between-Group Difference in Regional GM Loss

The locations and spatial extents of anatomical regions with significant differences in GMV between the 2 groups are presented in Table 2 and Figure 1. Compared with normal controls, patients with PD showed significantly smaller GMVs of the right amygdala, left hippocampal formation, bilateral insular cortex, bilateral caudate nucleus, bilateral cerebellar superior semilunar lobule, right fusiform gyrus, and left middle frontal gyrus, and no significantly larger GMV.

TABLE 1. Demographic Data of Patients With PD and Controls

Clinical Demographics	PD, n = 23	Control, n = 15	*P* Value
Age, y	61.04 ± 6.79	56.00 ± 8.95	0.214
Sex, M/F	6/17	5/10	0.450
GMV	506.90 ± 56.54	560.99 ± 28.22	**0.007***
WMV	532.26 ± 53.11	539.070 ± 60.796	0.374
TIV	1039.16 ± 96.71	1100.05 ± 86.47	0.711
Numbers of EPCs			
$CD133^+CD34^+$, %	0.067 ± 0.032	0.048 ± 0.032	**0.042***
KDR^+CD34^+, %	0.015 ± 0.018	0.005 ± 0.006	**0.048***
Cardiovascular autonomic parameters			
BRS	4.078 ± 2.245	8.382 ± 4.101	**0.001****
HRDB	6.361 ± 3.559	11.667 ± 6.889	**0.021***
LF	50.730 ± 22.631	55.829 ± 23.118	0.601
HF	49.269 ± 22.631	44.138 ± 23.077	0.598
LF/HF ratio	1.547 ± 1.253	2.187 ± 2.237	0.350
Disease duration, y	4.47 ± 4.80	–	–
Treatment duration, mo	21.43 ± 21.01	–	–
Current daily dosage, mg	339.34 ± 333.02	–	–
Disease severity scale			
UPDRS I	4.608 ± 3.299	–	–
UPDRS II	11.782 ± 7.409	–	–
UPDRS III	28.652 ± 14.446	–	–
UPDRS total	44.869 ± 23.977	–	–
Modified H&Y	2.413 ± 1.072	–	–
S&E	79.565 ± 15.805	–	–

BRS = baroreflex sensitivity, EPC = epithelial progenitor cell, F = female, GMV = gray matter volume, HF = high frequency, HRDB = heart rate response to deep breathing, KDR = kinase insert domain-conjugating receptor, LF = low frequency, M = male, modified H&Y = modified Hoehn and Yahr staging scale (most advanced stage is 5), PD = Parkinson disease, S&E = Schwab and England Activities of Daily Living Scale (minimum point is 0, suggesting the presence of vegetative functions only), TIV = total intracranial volume, UPDRS = Unified Parkinson Disease Rating Scale, WMV = white matter volume.

* $P < 0.05$.

** $P < 0.005$.Boldface indicates statistical significance (* $P < 0.05$, ** $P < 0.005$).

Between-Group Differences in Circulatory EPCs

The EPCs profiles of the participants are listed in Table 1. Consistent with previous findings,[32] patients with PD (compared with controls) exhibited higher $CD133^+CD34^+$ EPC % (mean ± SD: 0.067 ± 0.032 vs 0.048 ± 0.032; $P = 0.042$) and KDR^+CD34^+ EPC % (mean ± SD: 0.015 ± 0.018 vs 0.005 ± 0.006; $P = 0.048$).

Correlations of Cardiovascular Autonomic Parameters With GM Volume, Circulatory EPCs, and Treatment Duration

Consistent with our hypothesis, worse cardiovascular autonomic function was associated with smaller GMVs in selected brain regions, as shown in Table 3 and Figure 2. The decreased BRS was associated with smaller GMV of the left hippocampal formation ($r = 0.465$, $P = 0.004$), left caudate nucleus ($r = 0.423$, $P = 0.010$), and left cerebellar superior semilunar lobule ($r = 0.394$, $P = 0.017$). Furthermore, lower HRDB was associated with smaller GMV in the left hippocampal formation ($r = 0.493$, $P = 0.002$) and right insular cortex ($r = 0.364$, $P = 0.029$). Treatment duration was not significantly correlated with BRS ($r = 0.128$, $P = 0.581$) or GMVs (Table 3).

Additionally, levels of vascular and neuronal repair mediators and circulating EPCs were also correlated with deficits in certain brain regions (Table 3). Increased percentage of circulating $CD133^+CD34^+$ EPCs was associated with smaller GMV of the right amygdala ($r = -0.444$, $P = 0.007$), right ($r = -0.403$, $P = 0.015$) and left ($r = -0.401$, $P = 0.015$) insular cortex, right caudate nucleus ($r = -0.338$, $P = 0.044$), and left cerebellar superior semilunar lobule ($r = -0.369$, $P = 0.027$). Increased percentage of circulating KDR^+CD34^+ EPCs was associated with smaller GMV of the left hippocampal formation ($r = -0.344$, $P = 0.040$) and left caudate nucleus ($r = -0.336$, $P = 0.045$). Both decreased BRS and increased percentage of EPCs were associated with smaller GMV of the left hippocampal formation.

DISCUSSION

In the comparison with normal controls, patients exhibited worse cardiovascular autonomic function and increased levels of circulating EPCs. VBM showed that GMV of several brain regions was significantly smaller in PD. Furthermore, particular brain regions were associated with poor cardiovascular autonomic function and increased levels of circulating EPCs. This study is the first to show associations of autonomic function with smaller GMV and increased levels of circulatory EPCs in PD.

Decreased BRS and HRDB are both regarded as indications of autonomic dysfunction in PD. Variation in HRDB is an indicator of parasympathetic activity in the heart[1] and BRS is

TABLE 2. Regions Showing Gray Matter Volume Differences Between Patients With PD and Normal Controls

MNI Atlas Coordinates						GMV, mm^3		
X	Y	Z	Voxel Size	Gray Matter	BA	PD	Controls	t_{max}
27	4	−26	365	Amygdala, R	34	773.76 ± 114.58	950.83 ± 109.22	4.30
−24	−39	−17	613	Hippocampal formation, L	36	1561.10 ± 172.57	1860.72 ± 187.45	5.09
40	3	−12	706	Insular cortex, R	13	1513.19 ± 144.92	1744.21 ± 157.49	4.50
−38	3	−14	272	Insular cortex, L	13	603.71 ± 47.85	685.60 ± 63.93	4.60
12	10	−5	165	Caudate nucleus, R	–	421.42 ± 55.33	488.09 ± 48.96	3.82
−10	14	12	270	Caudate nucleus, L	–	480.99 ± 128.09	651.24 ± 141.24	4.08
36	−55	−44	193	Cerebellar superior semilunar lobule, R	–	341.27 ± 106.29	476.07 ± 88.09	3.89
−45	−46	−38	1104	Cerebellar superior semilunar lobule, L	–	2094.70 ± 450.91	2864.72 ± 457.27	5.05
38	−61	−17	188	Fusiform gyrus, R	37	356.65 ± 67.49	466.54 ± 83.93	4.15
−48	11	42	325	Middle frontal gyrus, L	6	575.06 ± 91.44	737.28 ± 117.76	4.50

BA = Brodmann area, GMV = gray matter volume, L = left side, MNI = Montreal Neurological Institute, PD = Parkinson disease, R = right side. The statistical criteria were set at joint voxel height uncorrected $P < 0.001$ and a cluster extent threshold of the family-wise error rate (P_{FWE}) < 0.05.

believed to be a reliable indicator of autonomic function. The ATRAMI study identified depressed BRS as an independent predictor of sudden cardiac death and life threatening arrhythmias and therefore at least partly responsible for increased mortality.[33]

Our results showing autonomic dysfunction in PD suggest an underlying degenerative process that affects the autonomic ganglia, brainstem nuclei, and hypothalamic nuclei.[1] Although impairment of both the central and the peripheral nervous systems contribute to autonomic dysfunction, central autonomic nervous system impairment may develop earlier in the disease course. The pathological evidence shows that Lewy body accumulation initially appears in the brainstem and adjacent neural structures and spreads to higher cortical areas as PD progresses.[34] Those brain regions are primarily responsible for heart rate modulation and autonomic function regulation.[35] Alterations of these cortical structures might interfere with central autonomic regulation in PD.

In the present study, patients with PD showed smaller GMVs in some parts of the central autonomic network, such as the amygdala, hippocampal formation, caudate, insula, and cerebellum, consistent with previous meta-analytic results.[9,10] Furthermore, the associations between autonomic dysfunction and particular brain anatomical abnormalities support our hypothesis

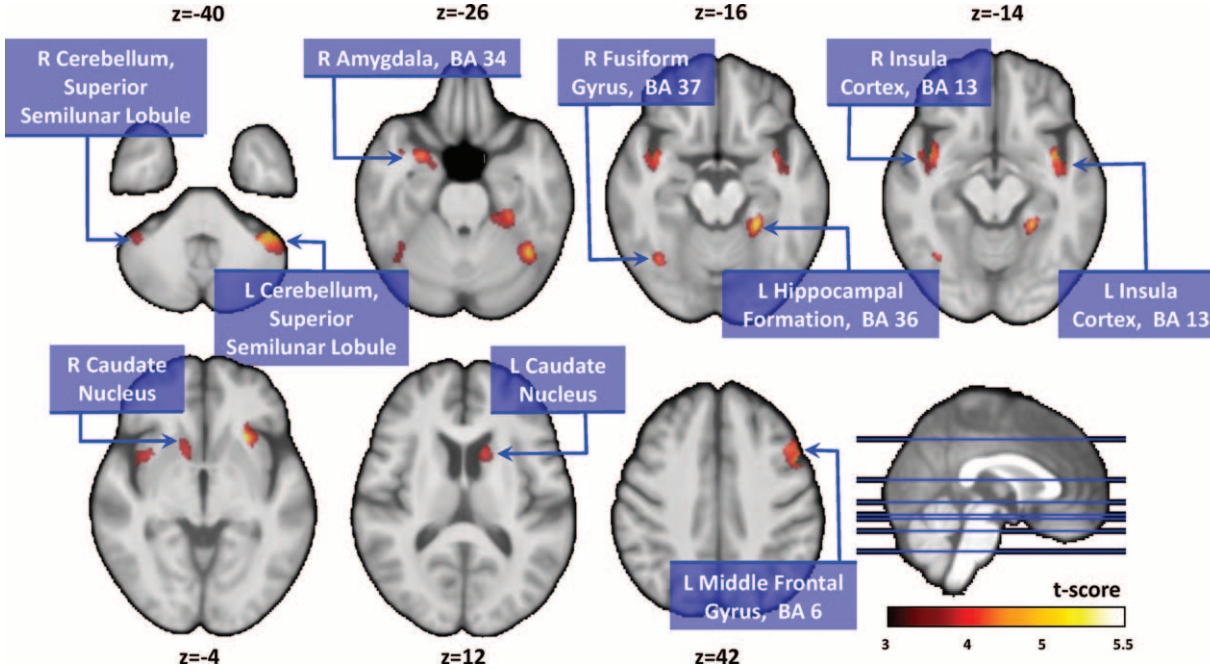

FIGURE 1. Compared with normal controls, patients with PD showed significantly smaller gray matter volumes in the right amygdala, left hippocampal formation, bilateral insular cortex, bilateral caudate nucleus, bilateral cerebellar superior semilunar lobule, right fusiform gyrus, and left middle frontal gyrus. PD = Parkinson disease.

TABLE 3. Correlations With Gray Matter Volume After Controlling for Age and Sex

	Cardiovascular Autonomic Parameters		Numbers of EPCs		
GMV Anatomical Location	**HRDB**	**BRS**	**$CD133^+CD34^+$, %**	**KDR^+CD34^+, %**	**Treatment Duration**
Amygdala (BA 34), R	0.261	0.260	**−0.444***	−0.242	−0.368
Hippocampal formation (BA 36), L	**0.493****	**0.465****	0.035	**−0.344***	−0.254
Insular cortex (BA 13), R	**0.364***	0.268	**−0.403***	−0.292	0.176
Insular cortex (BA 13), L	0.242	0.191	**−0.401***	−0.221	−0.053
Caudate nucleus, R	0.231	0.281	**−0.338***	−0.154	−0.119
Caudate nucleus, L	0.308	**0.423***	−0.135	**−0.336***	−0.042
Cerebellar superior semilunar lobule, R	0.329	0.243	−0.272	−0.236	0.256
Cerebellar superior semilunar lobule, L	0.321	**0.394***	**−0.369***	−0.122	0.047
Fusiform gyrus (BA 37), R	0.237	0.273	−0.193	−0.092	−0.014
Middle frontal gyrus (BA 6), L	0.290	0.225	−0.199	−0.308	0.411

BA = Brodmann area, BRS = baroreflex sensitivity, EPC = epithelial progenitor cell, GMV = gray matter volume, HRDB = heart rate response to deep breathing, KDR = kinase insert domain-conjugating receptor, L = left side, R = right side.

* $P < 0.05$.

** $P < 0.005$. Boldface indicates statistical significance (* $P < 0.05$, ** $P < 0.005$).

that the central autonomic network modulates clinical features of PD. The presence of a central autonomic network has been proposed previously and its functions investigated using somatosensory, cognitive, affective, and motor tasks.[36] Sympathetic regulation mainly involves the prefrontal cortex, cingulate, amygdala, insula, and cerebellum, while parasympathetic regulation involves the cingulate, caudate, temporal lobe, amygdala, insula, and hippocampal formation.[36] Our results were highly consistent with previous physiological findings.

Although very heterogeneous, the functions of the central autonomic network are well recognized. The amygdala is responsible for emotional processing and parasympathetic regulation to balance the sympathetic and parasympathetic responses to aversive stimuli.[36] The insula is a functionally heterogeneous structure[37] associated with sympathetic and parasympathetic activities separately.[36] The right anterior insula may be a sympathetic regulatory center[38] and heart rate input has been associated anatomically with the amygdala, hippocampus, insula, and cerebellum, further implicating these sites as autonomic control centers.[35] The high correlation between the GMV of the hippocampal formation and cardiovascular autonomic function (Figure 2) in the present study further supports the hypothesis that the hippocampus plays an important role in heart rate control[35] and parasympathetic regulation by the central autonomic network.[36] Our VBM results demonstrate that both the sympathetic and the parasympathetic components of the autonomic nervous system are affected as autonomic function worsens in PD.

An oxidative stress biomarker (i.e., level of circulating EPCs)[39] has been reported to increase in PD,[32] and increased oxidative stress has been reported to be its main etiology.[40] In our study, patients with PD simultaneously exhibited increased EPC levels and abnormalities of the central autonomic network, including the amygdala, hippocampal formation, insula, caudate, and cerebellum. Associations have been demonstrated between increased oxidative stress and enhanced susceptibility of brain tissue to oxidative damage[41] and between increased EPC level and sympathetic under-activity/parasympathetic over-activity.[42] Our results not only support that EPCs play a potential role in vascular repair and tissue healing[43] but also imply that the vascular and neuronal repair mediators proportionally compensate for the loss of brain volume as PD

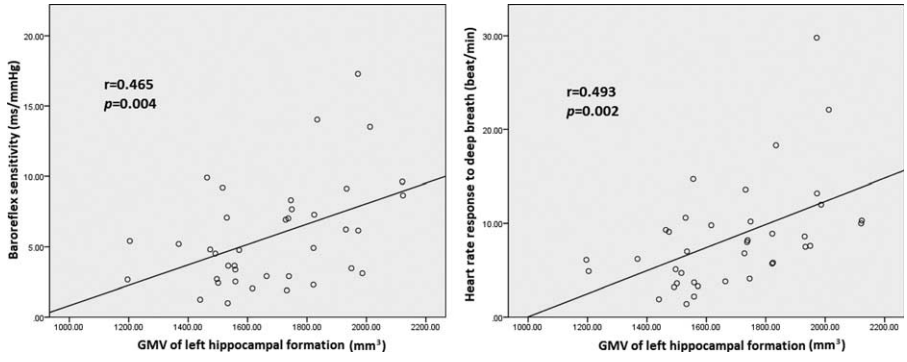

FIGURE 2. Smaller gray matter volume of the left hippocampal formation was associated with decrease in cardiovascular autonomic parameters (i.e., baroreflex sensitivity [$r = 0.465$, $P = 0.004$] and heart rate response to deep breathing [$r = 0.493$, $P = 0.002$]).

progresses. In the future, interactions between oxidative stress and brain microstructures should be studied directly using animal models.

Even though it produced significant evidence, this study still has limitations. First, the interpretation of results may be influenced by the relatively small sample size and variation in treatment duration. Further study including a larger number of patients with longitudinal evaluation of their clinical status should be carried out to test the conclusions of this study. Second, though the EPC findings were significant in the present study, peripheral EPC level can be affected by other oxidative stress biomarkers and uncontrollable confounders, such as underlying disease, physical activity, and substance abuse. The proximate cause should be carefully defined. Further studies may be needed to clarify the relationships among medications, autonomic dysfunction, and oxidative stress.

This study showed that, in PD, cardiovascular autonomic function is decreased, circulating EPC level is increased, and these changes are associated with smaller GMV of specific brain regions. We identified the left hippocampal formation as a bridge connecting the level of circulatory EPCs with BRS, and as a potential bio-target for monitoring disease progression and treatment efficacy in PD.

REFERENCES

1. Zesiewicz TA, Baker MJ, Wahba M, et al. Autonomic nervous system dysfunction in Parkinson's disease. *Curr Treat Options Neurol.* 2003;5:149–160.
2. Kim JB, Kim BJ, Koh SB, et al. Autonomic dysfunction according to disease progression in Parkinson's disease. *Parkinsonism Relat Disord.* 2014;20:303–307.
3. Friedrich C, Rudiger H, Schmidt C, et al. Baroreflex sensitivity and power spectral analysis during autonomic testing in different extrapyramidal syndromes. *Mov Disord.* 2010;25:315–324.
4. Holsen LM, Lee JH, Spaeth SB, et al. Brain hypoactivation, autonomic nervous system dysregulation, and gonadal hormones in depression: a preliminary study. *Neurosci Lett.* 2012;514:57–61.
5. Jellinger KA. Neuropathobiology of non-motor symptoms in Parkinson disease. *J Neural Transm.* 2015;122:1429–1440.
6. Muller CM, de Vos RA, Maurage CA, et al. Staging of sporadic Parkinson disease-related alpha-synuclein pathology: inter- and intra-rater reliability. *J Neuropathol Exp Neurol.* 2005;64:623–628.
7. Jubault T, Brambati SM, Degroot C, et al. Regional brain stem atrophy in idiopathic Parkinson's disease detected by anatomical MRI. *PLoS ONE.* 2009;4:e8247.
8. Obeso JA, Rodriguez-Oroz MC, Rodriguez M, et al. Pathophysiology of the basal ganglia in Parkinson's disease. *Trends Neurosci.* 2000;23:S8–S19.
9. Pan PL, Shi HC, Zhong JG, et al. Gray matter atrophy in Parkinson's disease with dementia: evidence from meta-analysis of voxel-based morphometry studies. *Neurol Sci.* 2013;34:613–619.
10. Shao N, Yang J, Shang H. Voxelwise meta-analysis of gray matter anomalies in Parkinson variant of multiple system atrophy and Parkinson's disease using anatomic likelihood estimation. *Neurosci Lett.* 2015;587:79–86.
11. Geha PY, Baliki MN, Harden RN, et al. The brain in chronic CRPS pain: abnormal gray-white matter interactions in emotional and autonomic regions. *Neuron.* 2008;60:570–581.
12. Hu W, Guo J, Chen N, et al. A meta-analysis of voxel-based morphometric studies on migraine. *Int J Clin Exp Med.* 2015;8:4311–4319.
13. Umeda S, Harrison NA, Gray MA, et al. Structural brain abnormalities in postural tachycardia syndrome: a VBM-DARTEL study. *Front Neurosci.* 2015;9:34.
14. Baev KV, Greene KA, Marciano FF, et al. Physiology and pathophysiology of cortico-basal ganglia-thalamocortical loops: theoretical and practical aspects. *Prog Neuropsychopharmacol Biol Psychiatry.* 2002;26:771–804.
15. Parent A, Hazrati LN. Functional anatomy of the basal ganglia. I. The cortico-basal ganglia-thalamo-cortical loop. *Brain Res Brain Res Rev.* 1995;20:91–127.
16. Conti FF, Brito Jde O, Bernardes N, et al. Cardiovascular autonomic dysfunction and oxidative stress induced by fructose overload in an experimental model of hypertension and menopause. *BMC Cardiovasc Disord.* 2014;14:185.
17. Hald A, Lotharius J. Oxidative stress and inflammation in Parkinson's disease: is there a causal link? *Exp Neurol.* 2005;193:279–290.
18. Cogle CR, Yachnis AT, Laywell ED, et al. Bone marrow transdifferentiation in brain after transplantation: a retrospective study. *Lancet.* 2004;363:1432–1437.
19. Zangiacomi V, Balon N, Maddens S, et al. Cord blood-derived neurons are originated from $CD133^{+}$/CD34 stem/progenitor cells in a cell-to-cell contact dependent manner. *Stem Cells Dev.* 2008;17:1005–1016.
20. Asahara T, Masuda H, Takahashi T, et al. Bone marrow origin of endothelial progenitor cells responsible for postnatal vasculogenesis in physiological and pathological neovascularization. *Circ Res.* 1999;85:221–228.
21. Beck H, Voswinckel R, Wagner S, et al. Participation of bone marrow-derived cells in long-term repair processes after experimental stroke. *J Cereb Blood Flow Metab.* 2003;23:709–717.
22. Hughes AJ, Daniel SE, Kilford L, et al. Accuracy of clinical diagnosis of idiopathic Parkinson's disease: a clinico-pathological study of 100 cases. *J Neurol Neurosurg Psychiatry.* 1992;55:181–184.
23. Gasser T, Bressman S, Durr A, et al. State of the art review: molecular diagnosis of inherited movement disorders. Movement Disorders Society task force on molecular diagnosis. *Mov Disord.* 2003;18:3–18.
24. Goetz CG, Poewe W, Rascol O, et al. Movement Disorder Society Task Force report on the Hoehn and Yahr staging scale: status and recommendations. *Mov Disord.* 2004;19:1020–1028.
25. Schwab RS, Engeland A. Projection technique for evaluating surgery in Parkinson's disease. In: Gillingham FJ, Donaldson MC, eds. *Third Symposium on Parkinson's Disease.* Edinburgh: Churchill Livingstone; 1969:152–157.
26. Tohka J, Zijdenbos A, Evans A. Fast and robust parameter estimation for statistical partial volume models in brain MRI. *NeuroImage.* 2004;23:84–97.
27. Rajapakse JC, Giedd JN, Rapoport JL. Statistical approach to segmentation of single-channel cerebral MR images. *IEEE Trans Med Imaging.* 1997;16:176–186.
28. Cuadra MB, Cammoun L, Butz T, et al. Comparison and validation of tissue modelization and statistical classification methods in T1-weighted MR brain images. *IEEE Trans Med Imaging.* 2005;24:1548–1565.
29. Bezzola L, Merillat S, Gaser C, et al. Training-induced neural plasticity in golf novices. *J Neurosci.* 2011;31:12444–12448.
30. Muhlau M, Winkelmann J, Rujescu D, et al. Variation within the Huntington's disease gene influences normal brain structure. *PLoS ONE.* 2012;7:e29809.
31. Ziegler G, Dahnke R, Jancke L, et al. Brain structural trajectories over the adult lifespan. *Hum Brain Mapp.* 2012;33:2377–2389.
32. Pezzoli G, Cavanna F, Cassani E, et al. Endothelial progenitor cells: cardiovascular protection in Parkinson's disease? *Int J Cardiol.* 2015;197:200–202.

33. Ziemssen T, Reichmann H. Cardiovascular autonomic dysfunction in Parkinson's disease. *J Neurol Sci.* 2010;289:74–80.

34. Braak H, Del Tredici K, Rüb U, et al. Staging of brain pathology related to sporadic Parkinson's disease. *Neurobiol Aging.* 2003;24:197–211.

35. Harper RM, Bandler R, Spriggs D, et al. Lateralized and widespread brain activation during transient blood pressure elevation revealed by magnetic resonance imaging. *J Comp Neurol.* 2000;417:195–204.

36. Beissner F, Meissner K, Bar KJ, et al. The autonomic brain: an activation likelihood estimation meta-analysis for central processing of autonomic function. *J Neurosci.* 2013;33:10503–10511.

37. Deen B, Pitskel NB, Pelphrey KA. Three systems of insular functional connectivity identified with cluster analysis. *Cereb Cortex.* 2011;21:1498–1506.

38. Cechetto DF, Shoemaker JK. Functional neuroanatomy of autonomic regulation. *NeuroImage.* 2009;47:795–803.

39. Case J, Ingram DA, Haneline LS. Oxidative stress impairs endothelial progenitor cell function. *Antioxid Redox Signal.* 2008;10:1895–1907.

40. Lin WC, Tsai NW, Huang YC, et al. Peripheral leukocyte apoptosis in patients with Parkinsonism: correlation with clinical characteristics and neuroimaging findings. *Biomed Res Int.* 2014;2014:635923.

41. Janowitz D, Wittfeld K, Terock J, et al. Association between waist circumference and gray matter volume in 2344 individuals from two adult community-based samples. *NeuroImage.* 2015;122:149–157.

42. de Cavanagh EM, Gonzalez SA, Inserra F, et al. Sympathetic predominance is associated with impaired endothelial progenitor cells and tunneling nanotubes in controlled-hypertensive patients. *Am J Physiol Heart Circ Physiol.* 2014;307:H207–H215.

43. Stellos K, Panagiota V, Sachsenmaier S, et al. Increased circulating progenitor cells in Alzheimer's disease patients with moderate to severe dementia: evidence for vascular repair and tissue regeneration? *J Alzheimers Dis.* 2010;19:591–600.